IDENTIFYING PATCHY SATURATION FROM WELL LOGS

JACK DVORKIN, DAN MOOS, JAMES PACKWOOD, AND AMOS NUR
DEPARTMENT OF GEOPHYSICS, STANFORD UNIVERSITY

INTRODUCTION

Gassmann's (1951) equations relate the elastic bulk (K_{Sat}) and shear (G_{Sat}) moduli of a fully-saturated rock to those of the dry rock frame (K_{Dry} and G_{Dry}, respectively), porosity φ, and the bulk moduli of the mineral phase (K_s) and pore fluid (K_f):

$$K_{Sat} = K_s \frac{\varphi K_{Dry} - (1+\varphi) K_f K_{Dry} / K_s + K_f}{(1-\varphi) K_f + \varphi K_s - K_f K_{Dry} / K_s}, \quad G_{Dry} = G_{Sat} \equiv G. \tag{1}$$

These equations are valid at low frequencies which, in most practical cases, include the seismic and sonic data ranges (the bounds for the low-frequency approximation are discussed in Mavko et al., 1998). Gassmann's equations are used for pore fluid identification from seismic and sonic because the elastic moduli are directly related to V_p and V_s:

$$V_p = \sqrt{(K_{Sat} + 4G/3)/\rho}, \quad V_s = \sqrt{G/\rho}, \tag{2}$$

where ρ is the bulk density.

When using Gassmann's equations at partial saturation, one has to calculate the effective bulk modulus of a fluid mixture in the pore space. One physically meaningful assumption is that wave-induced increments of pore pressure in each phase of the mixture equilibrate during a seismic period. This assumption leads to the isostress (Reuss) average for the effective bulk modulus of the mixture (e.g., gas-water):

$$K_f^{-1} = S_w K_w^{-1} + (1 - S_w) K_g^{-1}, \tag{3}$$

where S_w is water saturation; and K_w and K_g are the bulk moduli of water and gas, respectively. The condition of pore pressure equilibrium is satisfied if immiscible gas and water coexist at the pore scale, i.e., every pore contains S_w volumetric fraction of water and $1 - S_w$ fraction of gas. It can be also satisfied if gas and water occupy fully dry and fully saturated patches, respectively. However, the length-scale of such patches has to

be smaller than $\sqrt{\kappa K_w / f\mu}$, where κ is the permeability, f is the seismic frequency, and μ is the dynamic viscosity of water (Mavko and Mukerji, 1998). This upper bound applies to any multiphase mixture with K_w and μ being those of the most viscous phase. It can be on the order of a few millimeters at sonic frequencies and on the order of a meter at seismic frequencies. This state of partial saturation where Equation (3), together with Gassmann's equations, is applicable for calculating the rock's elastic moduli is "uniform" or "homogeneous" saturation (Mavko and Mukerji, 1998). Given that $K_g << K_w$, K_f, as calculated from Equation (3), remains much smaller than K_w at all saturations except those very close to 100%. Therefore, V_p remains practically insensitive to water saturation in the dominant part of its range (Figure 1). Domenico (1976 and 1977) seems to be the first to experimentally reproduce this effect. He also noticed that velocity (in sand and glass beads) may significantly deviate from the Equation (3) curve if saturation is heterogeneous.

To calculate the elastic moduli of rock with patchy saturation, consider a volume of rock at partial saturation S_w. The dry frame of the rock is elastically uniform within the volume. Let us assume that saturation is perfectly patchy, i.e., all water is concentrated in fully saturated patches, and gas is concentrated in patches with $S_w = 0$. This situation is perceived as a limiting case that may not necessarily be realized in rocks (since there is always residual water saturation in "dry" patches). At patchy saturation, Gassmann's equations can be separately applied to fully saturated and dry patches. The volume fraction of the former in the volume is S_w. The volume under examination includes regions with different bulk moduli but the same shear modulus. Then the effective bulk modulus K_{SatP} of the volume is (Hill, 1963):

$$(K_{SatP} + 4G/3)^{-1} = S_w(K_1 + 4G/3)^{-1} + (1 - S_w)(K_0 + 4G/3)^{-1}, \qquad (4)$$

where K_1 and K_0 are the bulk moduli of the rock at $S_w = 1$ and $S_w = 0$, respectively. At patchy saturation, V_p is very sensitive to S_w (Figure 1).

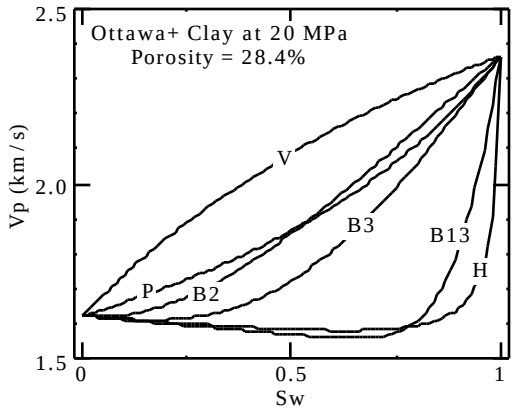

Figure 1. Velocity versus saturation for a sample that is an artificial mixture of Ottawa sand and kaolinite with 10% weight fraction of the latter (Yin, 1993). Porosity is 28.4%. At 20 MPa effective pressure, the dry-frame moduli of the rock are 2.637 GPa and 1.74 GPa for bulk and shear, respectively. The bulk moduli of gas and water are 0.033 GPa and 2.9 GPa, respectively. The curves are: "H" for homogeneous saturation; "P" for patchy saturation; "V" for Voigt fluid mixture as in Equation (5); "B2" for the Brie mixture with e = 2, as in Equation (6); "B3" for e = 3; and "B13" for e = 13. All curves are calculated from the dry-rock moduli using Equations (1), (2), (3), (4), (5) and (6).

At patchy saturation, Equations (1) cannot be applied to the entire rock volume because there is no such physical entity as uniform pore fluid. Still, mathematically a pore-fluid bulk modulus exists that, if substituted into Gassmann's equations, will yield any desired K_{SatP}. Domenico (1976) proposed to calculate this modulus of fictitious homogeneous pore fluid from the isostrain (Voigt) average:

$$K_f = S_w K_w + (1 - S_w) K_g. \qquad (5)$$

These values were close to the (fictitious) pore-fluid modulus back-calculated from the data using Gassmann's equations.

Brie et al. (1995) observed a deviation of the V_p / V_s ratio from typical homogeneous saturation values and attributed it to patchy saturation. To model this deviation, they used Gassmann's equations with an additional, ad-hoc expression for the bulk modulus of the fictitious uniform pore fluid:

$$K_f = (K_w - K_g) S_w^{\,e} + K_g, \qquad (6)$$

where e is a calibration parameter (Figure 1). By adjusting e, Brie et al. matched the in-situ data.

In this paper, we offer a ***first-principle-based*** (as opposed to ad-hoc) method for identifying patchy saturation in-situ. First we assume that saturation is homogeneous and use Equations (1), (2), and (3) to calculate the dry-frame bulk and shear moduli from V_p and V_s. Then we calculate the dry-frame Poisson's ratio as

$$\nu_{Dry} = 0.5(3K_{Dry} / G - 2) / (3K_{Dry} / G + 1). \quad (7)$$

We use ν_{Dry} as the criterion for patchy saturation: if its values, as calculated from in-situ data and the homogeneous saturation equations, exceed a reasonable experimentally-established threshold, saturation is patchy. In this case one has to further verify the existence of patchiness by obtaining reasonable ν_{Dry} from the patchy saturation equations. Once saturation type is established, saturation values can be calculated from sonic using the appropriate (homogeneous or patchy) set of equations. This routine eliminates the need for adjusting non-physical "free" parameters.

We apply this criterion to sonic data from a soft formation and identify a patchy saturation interval.

POISSON'S RATIO AS DISCRIMINATOR FOR SATURATION PATTERN

Dry-Frame Values

Spencer et al. (1994) report that at in-situ pressure many unconsolidated sands from the Gulf of Mexico have dry-frame Poisson's ratios near 0.18, while other Gulf Coast reservoirs have these values as low as 0.115. Only occasionally (among a large number of rock samples) does ν_{Dry} exceed 0.2, with the maximum value 0.237. To further support this fact, we present ν_{Dry} data at 20 MPa effective pressure reported by Han (1986) for consolidated sandstones; Jizba (1991) for tight gas sandstones; and Strandenes (1991) and Blangy (1992) for North Sea sandstones (Figure 2). All datasets include rocks with varying amounts of clay.

Most of the data points lie below 0.2. Only a few of them reach 0.25. In Figure 2a we also show a data point relevant to the case study below. This datum (Yin, 1993) is used

in Figure 1 (see description there). The sample is an artificial mixture of Ottawa sand and kaolinite with 10% weight fraction of the latter. Its ν_{Dry} is 0.23.

Based on these observations we choose 0.25 as an upper bound for ν_{Dry} in sands.

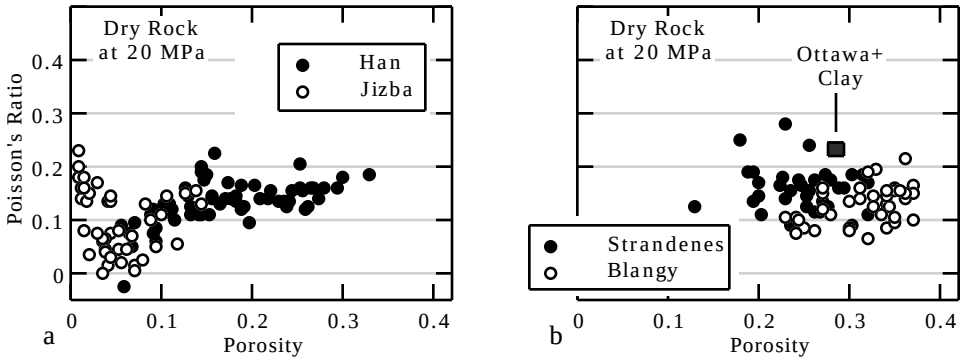

Figure 2. Dry-rock Poisson's ratio versus porosity for consolidated low-to-medium porosity sandstones (a); and high-porosity "fast" (Strandenes, 1991) and "slow" (Blangy, 1992) sands (b). The filled square in "b" is for Yin's (1993) data.

Identifying Patchy Saturation

In Figure 3a we plot the Poisson's ratio of the Ottawa/kaolinite sample (see above) versus saturation. The curves are computed from the dry-rock data at 20 MPa using homogeneous and patchy saturation equations. The difference between the "homogeneous" and "patchy" Poisson's ratio is drastic.

We take advantage of this difference in identifying the saturation pattern from measurements. Let us assume that the sample has patchy saturation and that the "measured" V_p and V_s are 1.8 and 0.934 km/s, respectively, at 40% saturation (Figure 1). The bulk density is 2.03 g/cm^3. Also, the measurements at other saturations are not available, and neither are the dry-frame elastic moduli of the rock. Given these "measured" values and the properties of the mineral and pore-fluid phases, we calculate the dry-frame elastic properties using the inverse of Equations (1)

$$K_{Dry} = K_s \frac{1-(1-\varphi)K_{Sat}/K_s - \varphi K_{Sat}/K_f}{1+\varphi-\varphi K_s/K_f - K_{Sat}/K_s}, \qquad (8)$$

with K_f given by Equation (3). The resulting ν_{Dry} is 0.316.

The mistake we made by choosing the "homogeneous" inversion becomes apparent because 0.316 significantly exceeds the upper bound of 0.25. The "patchy" inversion gives a reasonable value of 0.23. The "homogeneous" inversion, if applied to the patchy data, gives unreasonable ν_{Dry} values practically over the entire S_w range (Figure 3a). Therefore, we use ν_{Dry} calculated from data by "homogeneous" or "patchy" inversion as an indicator of a saturation pattern: if its values are unreasonable, the applied inversion is wrong and the saturation pattern is opposite to that assumed.

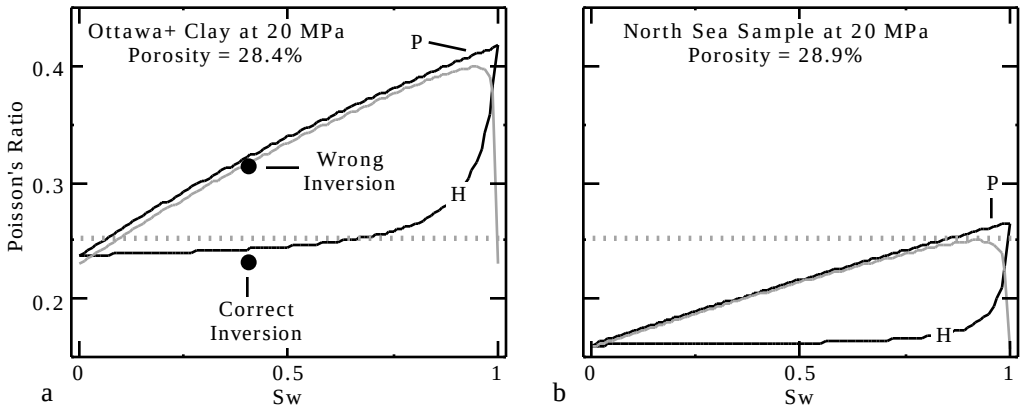

Figure 3. Poisson's ratio versus saturation. a. Soft Ottawa-kaolinite sample (Yin, 1993). b. Fast North Sea sample. Solid black curves are for the values calculated from the dry-frame moduli. "H" is for homogeneous and "P" is for patchy. Gray solid lines are for ν_{Dry} calculated from "patchy" data by "homogeneous" inversion. Gray dotted line is for the upper bound (0.25) of ν_{Dry}.

This method may fail for "fast" rocks. Consider a North Sea sample of 28.9% porosity with the dry-frame bulk and shear moduli 8.75 GPa and 7.69 GPa, respectively, at 20 MPa effective pressure (Strandenes, 1991). The calculated Poisson's ratio at partial saturation is given in Figure 3b. The "homogeneous" inversion applied to the "patchy" data produces wrong but reasonable ν_{Dry} values in the entire saturation range.

CASE STUDY

We examine open-hole log curves from a vertical well that penetrates unconsolidated and very soft gas sands. The frequency of the sonic tool is such that both P- and S-waves sample formation at the distance on the order of 1 m away from the well. The

shale content in the gas-saturated interval, as calculated from the gamma-ray curve, varies between 0.1 and 0.4. However, the clay content measured on cores is as low as 0.1 (Figure 4a). The total porosity and saturation were calculated by simultaneously solving the bulk-density equation and Archie's equation with the Humble formation factor formula for sands (Schlumberger, 1989). It is very close to the core porosity (Figure 4b). Water saturation may be as low as 0.2 (Figure 4c). The grain density was estimated as 2.64 g/cm^3 based on 10% clay content; the corresponding solid-phase bulk modulus is 34 GPa. The bulk moduli and densities of water and gas are 2.9 GPa and 0.033 GPa, and 1.055 g/cm^3 and 0.112 g/cm^3, respectively.

A question remains whether Archie's equation is applicable to estimating saturation from resistivity not only for the homogeneous but also for patchy saturation. We are not aware of any experimental data to refute or support our statement.

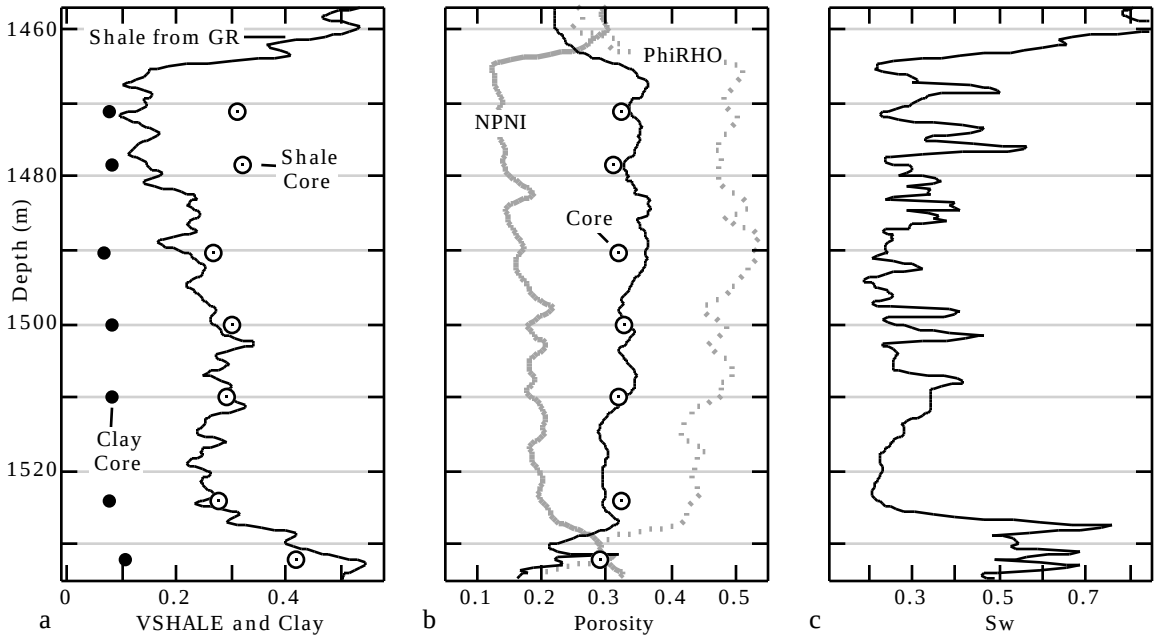

Figure 4. a. Shale and clay content versus depth. The curve is calculated from the gamma-ray data; symbols indicate core-measured values. Depth, as shown, is measured depth minus a constant. b. Neutron porosity (NPHI); porosity calculated from bulk density (PhiRHO); total porosity (solid black curve); and core-measured porosity. c. Water saturation.

The measured V_p and V_s are plotted versus porosity in Figure 5. We also plot the velocities for the North Sea high-porosity samples, and the Ottawa and kaolinite sample, all at 20 MPa effective pressure (the approximate effective pressure in the well) and 25% saturation for comparison. The North Sea velocities significantly exceed those in the well. However, the mixture of Ottawa sand and 10% kaolinite is elastically very close to the gas-saturated formation.

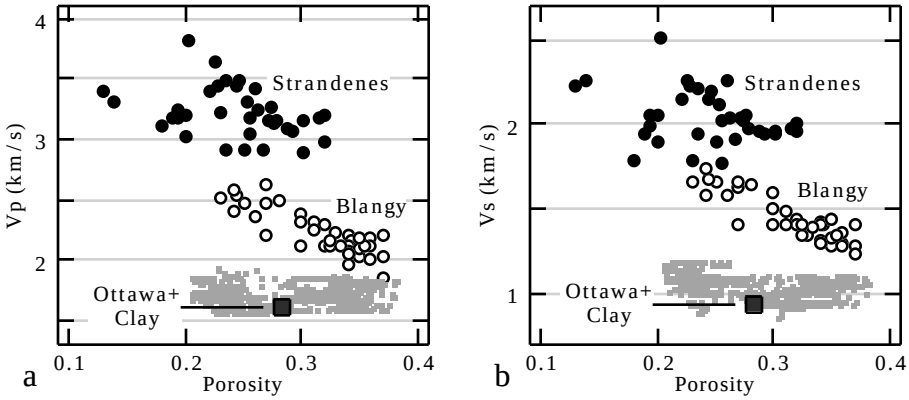

Figure 5. Velocity versus total porosity. Gray symbols are for this case study.

To calculate ν_{Dry} (Figure 6a), we separately use the "homogeneous" and "patchy" inversion (the latter directly follows from Equation (4) and is described in Dvorkin and Nur, 1998). An indirect indication of patchy saturation between 1495 m and 1520 m is the unreasonably high dry-frame "homogeneous" ν_{Dry}. The "patchy" ν_{Dry} only slightly exceeds the 0.25 upper bound and remains within reasonable limits.

The other possible interval with patchy saturation is between 1480 and 1490 m. Although the "homogeneous" inversion gives ν_{Dry} that is below 0.25, the "patchy" ν_{Dry} has lower and more reasonable values.

To illustrate the importance of identifying patchy saturation in situ, we calculate the dry-frame bulk modulus at the well. If saturation is assumed to be homogeneous (common fluid-substitution approach), the errors in K_{Dry} may exceed 50% (Figure 6b). Such errors have to be taken into account, as they may strongly affect seismic interpretation for direct hydrocarbon indication.

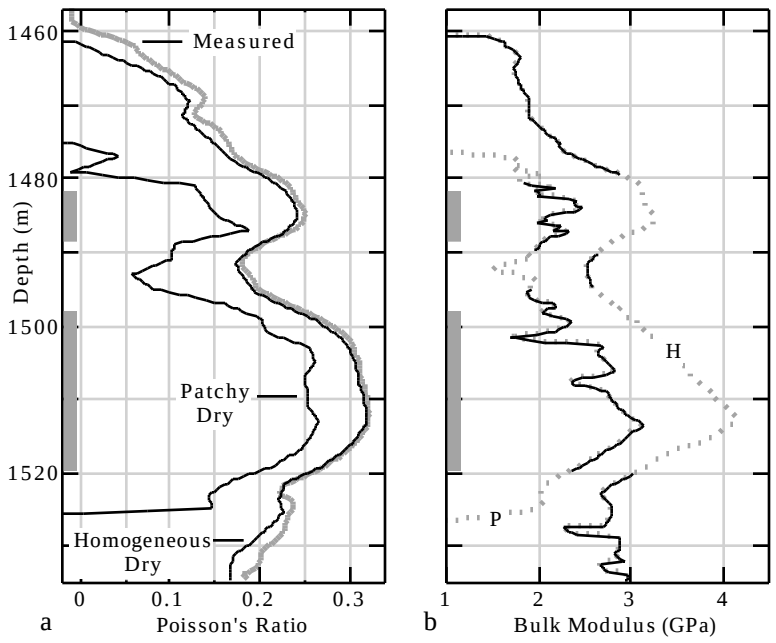

Figure 6. a. Poisson's ratio versus depth (measured depth minus a constant as in Figure 4). Bold gray curve is for measured Poisson's ratio. Black curves are for "homogeneous" and "patchy" ν_{Dry}. Vertical bars indicate likely intervals with patchy saturation. b. Dry-frame bulk modulus corrected for patchy saturation (solid black curve). Dotted curves are for homogeneous (H) and patchy (P) inversion.

DISCUSSION AND CONCLUSION

This case study shows that patchy saturation can be detected in situ using the dry-frame Poisson's ratio (calculated from data) as a discriminator. Both homogeneous and patchy saturation models have to be treated as idealized end members (or bounds) for a realistic situation. The fact is that where one of these two fluid substitution methods fails to give reasonable elastic moduli values for the dry frame, the other may do so. We suggest that in unconsolidated partially-saturated sands two fluid substitution techniques -- homogeneous and patchy -- be used to calculate the dry-rock elastic moduli from well logs. If the homogeneous inversion gives dry-rock Poisson's ratios which exceed 0.2 - 0.25, and at the same time the patchy inversion gives lower and more reasonable values, the interval is likely to be patchy-saturated. Then the dry-rock bulk moduli have to be calculated accordingly. We recommend using both techniques for bounding the possible dry-rock Poisson ratio and bulk modulus values.

The solution given in this paper shows that there is no need for introducing ad-hoc non-physical models with adjustable "free" parameters. Patchy saturation can be identified and quantitatively interpreted using rigorous equations.

REFERENCES

Blangy, J.P., 1992, Integrated seismic lithologic interpretation: The petrophysical basis: Ph.D. thesis, Stanford University.

Brie, A., Pampuri, F., Marsala, A.F., and Meazza, O., 1995, Shear sonic interpretation in gas-bearing sands: SPE 30595, 701-710.

Domenico, S.N., 1976, Effect of brine-gas mixture on velocity in an unconsolidated gas reservoir: Geophysics, **41**, 882-894.

Domenico, S.N., 1977, Elastic properties of unconsolidated porous sand reservoirs: Geophysics, **42**, 1339-1368.

Dvorkin, J., and Nur, A., 1998, Acoustic signatures of patchy saturation: Int. J. Solids and Structures, 35, 4803-4810.

Gassmann, F., 1951, Elasticity of porous media: Uber die elastizitat poroser medien: Vierteljahrsschrift der Naturforschenden Gesselschaft, **96**, 1-23.

Han, D.-H., 1986, Effects of porosity and clay content on acoustic properties of sandstones and unconsolidated sediments: Ph.D. thesis, Stanford University.

Hill, R., 1963, Elastic properties of reinforced solids: Some theoretical principles, J. Mech. Phys. Solids, **11**, 357-372.

Jizba, D., 1991, Mechanical and acoustical properties of sandstones and shales: Ph.D. thesis, Stanford University.

Mavko, G., Mukerji, T., and Dvorkin, J., 1998, The rock physics handbook: Cambridge University Press.

Mavko, G., and Mukerji, T., 1998, Bounds on low-frequency seismic velocities in partially saturated rocks: Geophysics, **63**, 918-924.

Schlumberger, 1989, Log interpretation principles/applications: Schlumberger Wireline & Testing, Houston.

Spencer, J.W., Cates, M.E., and Thompson, D.D., 1994, Frame moduli of unconsolidated sands and sandstones: Geophysics, **59**, 1352-1361.

Strandenes, S., 1991, Rock physics analysis of the Brent Group reservoir in the Oseberg Field: Stanford Rock Physics and Borehole Geophysics Project.

Yin, H., 1993, Acoustic velocity and attenuation of rocks: isotropy, intrinsic anisotropy, and stress induced anisotropy: Ph.D. thesis, Stanford University.